SOFTWARE NOTE

XEDA, a fast and multipurpose energy decomposition analysis program

Zhen Tang | Yanlin Song | Shu Zhang | Wei Wang | Yuan Xu | Di Wu |
Wei Wu [ORCID] | Peifeng Su [ORCID]

The State Key Laboratory of Physical Chemistry of Solid Surfaces, Fujian Provincial Key Laboratory of Theoretical and Computational Chemistry, and College of Chemistry and Chemical Engineering, Xiamen University, Xiamen, China

Correspondence
Wei Wu and Peifeng Su, The State Key Laboratory of Physical Chemistry of Solid Surfaces, Fujian Provincial Key Laboratory of Theoretical and Computational Chemistry, and College of Chemistry and Chemical Engineering, Xiamen University, Xiamen, Fujian 361005, China.
Email: weiwu@xmu.edu.cn (W. W.) and supi@xmu.edu.cn (P. S.)

Funding information
National Natural Science Foundation of China, Grant/Award Numbers: 21733008, 21973077; New Century Excellent Talents in Fujian Province University

Abstract

A fast and multipurpose energy decomposition analysis (EDA) program, called XEDA, is introduced for quantitative analysis of intermolecular interactions. This program contains a series of variational EDA methods, including LMO-EDA, GKS-EDA and their extensions, to analyze non-covalent interactions and strong chemical bonds in various environments. XEDA is highly efficient with a similar computational scaling of single point energy calculations. Its efficiency and universality are validated by a series of test examples including van der Waals interactions, hydrogen bonds, radical–radical interactions and strong covalent bonds.

1 | INTRODUCTION

Energy decomposition analysis (EDA) methods have been widely used for the quantitative analysis of intermolecular interactions based on quantum mechanical calculations.[1–12] They divide total interaction energies of molecular systems into several physically meaningful components to explore the physical origin of intermolecular interactions. Over the past decades, lots of EDA methods have been proposed, which can be classified into three groups, perturbation EDA methods,[4–8] variational EDA methods,[9–34] and real-space EDA methods.[35–37]

In 2009, a variational EDA method, named localized molecular orbitals-based EDA (LMO-EDA) was proposed by one of the present authors and coworker.[22] LMO-EDA can be used for exploring different weak and strong interactions by using Hartree–Fock (HF) and Kohn–Sham (KS) orbitals. To consider various interactions in complex systems, following LMO-EDA,[22] energy decomposition analysis with polarizable continuum model (EDA-PCM),[24] generalized Kohn–Sham energy decomposition analysis (GKS-EDA),[25] and their extensions, have been proposed in the last decade. EDA-PCM was developed for intermolecular interactions in the solvated

environments. GKS-EDA is an improved version of LMO-EDA, overcoming some shortcomings when KS orbitals are applied. Recently, a new extension of GKS-EDA, named GKS-EDA(BS),[33] was presented for intermolecular interactions in open shell singlet (OSS) states, which are challenging for most of EDA methods due to the multi-reference character. These EDA methods are capable of handling various chemical problems, which were comprehensively reviewed in a recently published article.[11]

Currently, the EDA methods mentioned above are implemented in various quantum chemical programs. For example, KM-EDA,[13] RVS-EDA,[17,18] and LMO-EDA[22] are included in the released version of GAMESS program;[38] ETS-NOCV-EDA[21] is implemented in ADF;[39] ALMO-EDA[20] is provided by Q-Chem.[40] Local-EDA[27] is available in ORCA.[41] SAPT[4–8] is involved in Q-Chem,[40] PSI4,[42] MOLPRO,[43] CamCASP,[44] and SAPT2020.[45] Our developed EDA methods were implemented in a home-made version of GAMESS.[38] Most recently, the GKS-EDA method has been implemented in Turbomole,[46] and used for the study of interactions in isoquinolinyl pyrazolate Pt(II) complexes.[47]

Recently, all our developed EDA methods were re-implemented as a novel program, named XEDA. Here X denotes

"Xiamen," a city in the southeast of China. The aim of XEDA is to provide users with a friendly and multipurpose tool for non-covalent interactions and strong covalent bonding interactions in various environments. In XEDA, algorithms are fully optimized, and thus memory requirement and computational cost are greatly reduced, compared to the previous version. This article concisely describes the GKS-EDA method and its relatives implemented in the current version of XEDA.

2 | THEORETICAL BACKGROUNDS

2.1 | GKS-EDA method

By using the generalized Kohn–Sham scheme theory,[48,49] GKS-EDA divides the total interaction energy into electrostatic (ΔE^{ele}), exchange-repulsion (ΔE^{exrep}), polarization (ΔE^{pol}), correlation (ΔE^{corr}) and dispersion (ΔE^{disp}) terms on the basis of KS-DFT calculations:[25]

$$\Delta E^{\text{TOT}} = \Delta E^{\text{ele}} + \Delta E^{\text{exrep}} + \Delta E^{\text{pol}} + \Delta E^{\text{corr}} + \Delta E^{\text{disp}}, \tag{1}$$

where the individual terms are defined as:

$$\Delta E^{\text{ele}} = \sum_{i\in\phi_0}^{\alpha,\beta} \langle i|h|i\rangle + \frac{1}{2}\sum_{i\in\phi_0}^{\alpha,\beta}\sum_{j\in\phi_0}^{\alpha,\beta} \langle ij|ij\rangle + E_S^{\text{nuc}}$$
$$- \sum_A \left(\sum_{i\in\phi_A}^{\alpha,\beta} \langle i|h|i\rangle + \frac{1}{2}\sum_{i\in\phi_A}^{\alpha,\beta}\sum_{j\in\phi_A}^{\alpha,\beta} \langle ij|ij\rangle + E_A^{\text{nuc}} \right), \tag{2}$$

where E^{nuc} is the nuclear repulsion energy; indices i and j denote all the occupied α and β Kohn–Sham (KS) orbitals; ϕ_A is the occupied orbitals of monomer A, and ϕ_0 is the sum of the all occupied orbitals of monomers. ϕ_0 is the direct product of monomers' wavefunction.

The exchange-repulsion term (ΔE^{exrep}) denotes the Pauli repulsion between monomers, which can be defined as:

$$\Delta E^{\text{exrep}} = -\frac{1}{2}\sum_A \left(\sum_{i\in\phi_A}^{\alpha}\sum_{j\neq\phi_A}^{\alpha} \langle ij|ji\rangle + \sum_{i\in\phi_A}^{\beta}\sum_{j\neq\phi_A}^{\beta} \langle ij|ji\rangle \right)$$
$$+ \sum_{i\in\phi_0}^{\alpha,\beta}\sum_{j\in\phi_0}^{\alpha,\beta} \langle i|h|j\rangle (S_{ij}^{-1} - \delta_{ij})$$
$$+ \frac{1}{2}\sum_{i\in\phi_0}^{\alpha,\beta}\sum_{j\in\phi_0}^{\alpha,\beta}\sum_{k\in\phi_0}^{\alpha,\beta}\sum_{l\in\phi_0}^{\alpha,\beta} \langle ij|kl\rangle (S_{ik}^{-1}S_{jl}^{-1} - \delta_{ik}\delta_{jl})$$
$$- \frac{1}{2}\left[\sum_{i\in\phi_0}^{\alpha}\sum_{j\in\phi_0}^{\alpha}\sum_{k\in\phi_0}^{\alpha}\sum_{l\in\phi_0}^{\alpha} \langle ij|kl\rangle (S_{ik}^{-1}S_{jl}^{-1} - \delta_{ik}\delta_{jl}) \right.$$
$$\left. + \sum_{i\in\phi_0}^{\beta}\sum_{j\in\phi_0}^{\beta}\sum_{k\in\phi_0}^{\beta}\sum_{l\in\phi_0}^{\beta} \langle ij|kl\rangle (S_{ik}^{-1}S_{jl}^{-1} - \delta_{ik}\delta_{jl}) \right], \tag{3}$$

where S_{ij}^{-1} is the inverse of the overlap between orbitals i and j.

The polarization term (ΔE^{pol}) shows the contribution of orbital relaxation from ϕ_0 to supermolecule's wavefunction, ϕ_S.

$$\Delta E^{\text{pol}} = \sum_{i\in\phi_S}^{\alpha,\beta} \langle i|h|i\rangle + \frac{1}{2}\sum_{i\in\phi_S}^{\alpha,\beta}\sum_{j\in\phi_S}^{\alpha,\beta} \langle ij|ij\rangle - \frac{1}{2}\left(\sum_{i\in\phi_S}^{\alpha}\sum_{j\in\phi_S}^{\alpha} \langle ij|ji\rangle + \sum_{i\in\phi_S}^{\beta}\sum_{j\in\phi_S}^{\beta} \langle ij|ji\rangle \right)$$
$$- \left[\begin{array}{l} \sum_{i\in\phi_0}^{\alpha,\beta}\sum_{j\in\phi_0}^{\alpha,\beta} \langle i|h|j\rangle S_{ij}^{-1} + \frac{1}{2}\sum_{i\in\phi_0}^{\alpha,\beta}\sum_{j\in\phi_0}^{\alpha,\beta}\sum_{k\in\phi_0}^{\alpha,\beta}\sum_{l\in\phi_0}^{\alpha,\beta} \langle ij|kl\rangle S_{ik}^{-1}S_{jl}^{-1} \\ -\frac{1}{2}(\sum_{i\in\phi_0}^{\alpha}\sum_{j\in\phi_0}^{\alpha}\sum_{k\in\phi_0}^{\alpha}\sum_{l\in\phi_0}^{\alpha} \langle ij|kl\rangle S_{ik}^{-1}S_{jl}^{-1} + \sum_{i\in\phi_0}^{\beta}\sum_{j\in\phi_0}^{\beta}\sum_{k\in\phi_0}^{\beta}\sum_{l\in\phi_0}^{\beta} \langle ij|kl\rangle S_{ik}^{-1}S_{jl}^{-1}) \end{array} \right], \tag{4}$$

The correlation term (ΔE^{corr}) is expressed as:

$$\Delta E^{\text{corr}} = E_S^{\text{corr}} - \sum_A E_A^{\text{corr}}, \tag{5}$$

where E_S^{corr} and E_A^{corr} are the GKS correlation energies of super-molecule and monomers A, respectively. They are defined as:

$$E_P^{\text{corr}} = (1-a)\left[E_X\left(\rho_P^\alpha, \rho_P^\beta\right) + \frac{1}{2}\left(\sum_{i\in\phi_P}^{\alpha}\sum_{j\in\phi_P}^{\alpha} \langle ij|ji\rangle + \sum_{i\in\phi_P}^{\beta}\sum_{j\in\phi_P}^{\beta} \langle ij|ji\rangle \right) \right]$$
$$+ E_C\left(\rho_P^\alpha, \rho_P^\beta\right). \tag{6}$$

Here $P = S$ or A. a is the hybrid coefficient (the portion of HF exchange in a hybrid functional), while $E_X\left(\rho_P^\alpha, \rho_P^\beta\right)$ and $E_C\left(\rho_P^\alpha, \rho_P^\beta\right)$ are the exchange and correlation energy of a DFT functional with the α and β spin density.

Dispersion term (ΔE^{disp}) is optional for dispersion correction DFT. It is computed as the difference of dispersion energies between the super-molecule and its monomers. To facilitate the discussions for various DFT functionals, ΔE^{corr} and ΔE^{disp} can be grouped as $\Delta E^{\text{corr/disp}}$ term in practice.

2.2 | GKS-EDA(BS)

GKS-EDA(BS) is an extension of GKS-EDA for intermolecular interactions in OSS states.[33] Based on BS-UDFT calculations with spin projection approximation,[50,51] GKS-EDA(BS) divides the total interaction energy into the following terms:

$$\Delta E_{\text{GS}}^{\text{TOT}} = \Delta E_{\text{GS}}^{\text{ele}} + \Delta E_{\text{GS}}^{\text{exrep}} + \Delta E_{\text{GS}}^{\text{pol}} + \Delta E_{\text{GS}}^{\text{corr}} + \Delta E_{\text{GS}}^{\text{disp}}, \tag{7}$$

The analysis result is the linear combination of total interaction energies and the EDA terms in high spin (HS) state and the broken symmetry low spin (BS) state, as

$$\Delta E_{\text{GS}}^{\text{X}} = (1+c)\Delta E_{\text{BS}}^{\text{X}} - c\Delta E_{\text{HS}}^{\text{X}}, \tag{8}$$

where $\Delta E_{\text{BS}}^{\text{X}}$ and $\Delta E_{\text{HS}}^{\text{X}}$ are interaction terms in BS state and HS state, respectively. Here X can be electrostatic, exchange-repulsion, polarization, correlation, and dispersion, respectively. To perform a GKS-EDA(BS) calculation, the direct product ϕ_0 in Equations (2)–(4) is

replaced by the broken symmetry form ϕ_0^{BS} and the high spin form ϕ_0^{HS}.

By using Yamaguchi projection scheme,[50] c is defined as:

$$c = \frac{\left\langle \hat{S}^2 \right\rangle_{BS}}{\left\langle \hat{S}^2 \right\rangle_{HS} - \left\langle \hat{S}^2 \right\rangle_{BS}}. \qquad (9)$$

Compared to GKS-EDA, no additional term is required. If $c = 0$, these definitions are the same with the GKS-EDA ones.

2.3 | LMO-EDA

The LMO-EDA method was mainly designed for HF and post-HF calculations, though it might be used for KS-DFT calculations. Based on post-HF calculations, LMO-EDA decomposes the total interaction energy into electrostatic (ΔE^{ele}), exchange-repulsion (ΔE^{exrep}), polarization (ΔE^{pol}), and correlation (ΔE^{corr}) terms.[22]

$$\Delta E^{TOT} = \Delta E^{ele} + \Delta E^{exrep} + \Delta E^{pol} + \Delta E^{corr}. \qquad (10)$$

Note that the last term ΔE^{corr} will not appear for Hartree Fock (HF) calculation. Definitions of electrostatic, exchange-repulsion, and polarization terms in LMO-EDA are the same with their corresponding terms in GKS-EDA except that KS orbitals are replaced by HF orbitals. The correlation term, which is defined as dispersion term in the original LMO-EDA paper, arises from the calculations with post-HF methods, for example, second order Møller–Plesset perturbation theory (MP2)[52] or coupled cluster methods (CC).[53,54] This term is defined as the difference between post-HF and HF interaction energies, showing the contribution of dynamic correlation to the total interaction energy.

2.4 | GKS-EDA(sol) and EDA-PCM

GKS-EDA(sol)[25] and EDA-PCM[24] are the extensions of GKS-EDA and LMO-EDA, respectively, for intermolecular interactions in solution phase. In GKS-EDA(sol) and EDA-PCM, implicit solvation models are employed to take the influence of long range solvent effects into account. The total interaction free energy is expressed as:

$$\Delta G^{TOT} = \Delta G^{ele} + \Delta G^{exrep} + \Delta G^{pol} + \Delta G^{corr} + \Delta G^{disp} + \Delta G^{desol}, \qquad (11)$$

for GKS-EDA(sol), and

$$\Delta G^{TOT} = \Delta G^{ele} + \Delta G^{exrep} + \Delta G^{pol} + \Delta G^{corr} + \Delta G^{desol}, \qquad (12)$$

for EDA-PCM.

In Equations (11) and (12), except ΔG^{desol}, the other terms are the same as the corresponding terms in GKS-EDA, GKS-EDA(BS) and LMO-EDA, but the orbitals used in these terms are optimized by the
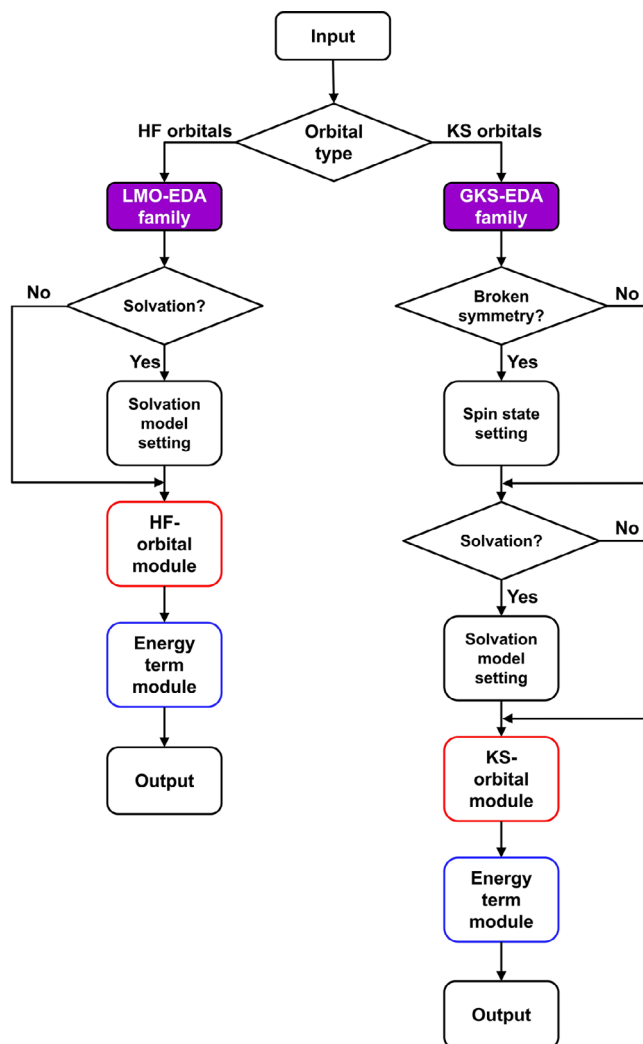

FIGURE 1 The flowchart of XEDA program

self-consistent reaction field (SCRF)[55–57] in polarizable continuum model (PCM).[58–60] ΔG^{desol} is defined as the difference of solute-solvent interacting energy from monomers' reaction fields to complex's reaction field. It should be noticed that ΔG^{desol} depends on the monomers' distance, not simply on the solvation free energy difference between supermolecule and monomers.[24]

3 | XEDA PROGRAM AND ITS FEATURES

The flowchart of XEDA is shown in Figure 1. The GKS-EDA family (GKS-EDA, GKS-EDA(sol), GKS-EDA(BS)) employs KS orbitals, while the LMO-EDA family (LMO-EDA and EDA-PCM) uses HF orbitals. The code is mainly composed of the orbital module and energy term module. The orbital module is designed for providing KS/HF orbitals of monomers and supermolecule for each step. All various wavefunctions required in XEDA can be constructed by two ways: reading from an input file or generating from a SCF procedure of orbital optimizations. Currently, the orbital module supports the SCF module of GAMESS.[38]
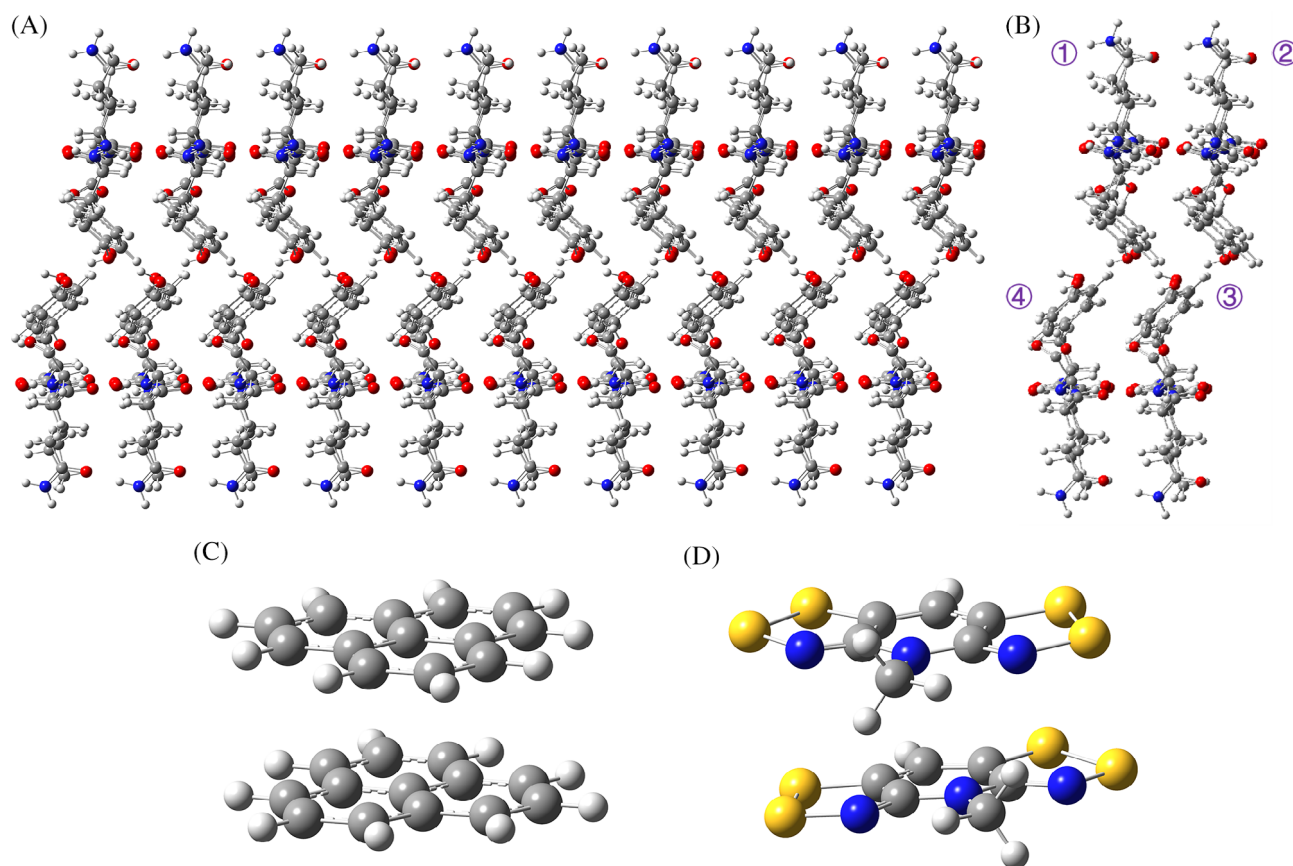
FIGURE 2   The geometries of the testing systems. (A) $(C_{33}H_{45}O_{10}N_7)_{10}...(C_{33}H_{45}O_{10}N_7)_{10}$; (B) $(C_{33}H_{45}O_{10}N_7)_4$; (C) PLY dimer; (D) BTA· dimer. C, O, N, H, and S atoms are in gray, red, blue, white, and yellow, respectively

The energy term module is designed for computing the energy components by using the wavefunction transferred from the orbital module. EDA terms can be computed as the energy difference between different energy of wavefunction. To compute the energy term, the module reads the integrals from the other quantum chemical programs. Electrostatic, exchange-repulsion, polarization, and correlation terms depend on the energy of single determinant in each step only; for the desolvation term, the energy module in the current version employs the solvation computation procedure in GAMESS to compute the solvation free energies in different steps. In this version, the computations of correlation and desolvation terms will link the DFT module (for GKS-EDA), post-HF module (for LMO-EDA) and solvation module in GAMESS.

The XEDA program shares the following features:

1. XEDA calculations can be performed with various kinds of orbitals, including restricted closed shell, restricted and unrestricted open shell orbitals.
2. In GKS-EDA, various DFT functionals, such as LDA, GGA, meta-GGA, hybrid, double hybrid, range-separated, and dispersion correction, can be employed.
3. LMO-EDA in XEDA is designed to perform with HF orbitals only. In LMO-EDA, various post-HF methods, for example, second order Møller–Plesset perturbation theory[52] or coupled cluster methods,[53,54] can be used.

4. For GKS-EDA(sol) and EDA-PCM, various implicit solvation models, including C-PCM,[61,62] IEF-PCM,[63–66] HET-CPCM,[67] and SMD,[68] can be employed.

4 | EXAMPLES

The test examples include benzene dimer, water dimer and amyloid-like IYQYGG segment (PDB code: 6G8C, denoted as $(C_{33}H_{45}O_{10}N_7...$ $C_{33}H_{45}O_{10}N_7)_{10})$[69,70] in gas phase, ammonia-water dimer in the aqueous solution; phenalenyl (PLY) dimer, π-stacked bis-dithiazolyl radical (BTA·) dimer; and the triple bonding interactions in a series of complexes including N_2, P_2, As_2, CO, NO, $CH \equiv CH$, La_2, and Ac_2, which are shown in Figure 2, are selected as examples.

GKS-EDA calculations are performed by using B3LYP-D3(BJ),[71,72] ωB97X-D,[73] and PBE,[74] which are the representative hybrid, range separated, and GGA functionals, respectively. They are widely used in non-covalent interactions and covalent bonds. The LMO-EDA calculations are carried at the MP2 level.[52] For EDA-PCM and GKS-EDA(sol) calculations, conductor-like polarizable continuum model (CPCM)[61,62] is employed. The Boys and Bernardi style counterpoise correction is used for correcting the basis set superposition errors (BSSE).[75]

The geometry of IYQYGG segment is taken from literature,[70] while the others are fully optimized by Gaussian 16 program.[76] For

TABLE 1 The GKS-EDA results of benzene dimer and water dimer at the B3LYP-D3/CCX and B3LYP-D3/ACCX level (X = D, T, Q, 5 and 6). Energy unit is kcal/Mol

B3LYP-D3		ΔE^{elec}	ΔE^{exrep}	ΔE^{pol}	ΔE^{disp}	ΔE^{corr}	ΔE^{TOT}
Benzene dimer	CCD	−3.65	9.08	−1.59	−4.78	−1.35	−2.29
	CCT	−3.53	9.14	−1.72	−4.78	−1.40	−2.29
	CCQ	−3.50	9.15	−1.74	−4.78	−1.41	−2.28
	CC5	−3.47	9.16	−1.74	−4.78	−1.41	−2.24
	CC6	−3.47	9.16	−1.74	−4.78	−1.42	−2.25
	ACCD	−3.48	9.18	−1.72	−4.78	−1.36	−2.16
	ACCT	−3.48	9.17	−1.74	−4.78	−1.42	−2.25
	ACCQ	−3.47	9.17	−1.74	−4.78	−1.42	−2.25
	ACC5	−3.47	9.16	−1.74	−4.78	−1.42	−2.25
	ACC6	−3.47	9.16	−1.73	−4.78	−1.43	−2.25
Water dimer	CCD	−9.37	8.81	−2.66	−0.63	−1.31	−5.17
	CCT	−8.70	8.31	−2.74	−0.63	−1.39	−5.15
	CCQ	−8.49	8.13	−2.79	−0.63	−1.38	−5.16
	CC5	−8.38	8.03	−2.83	−0.63	−1.36	−5.16
	CC6	−8.34	8.01	−2.84	−0.63	−1.36	−5.16
	ACCD	−8.31	8.02	−2.84	−0.63	−1.29	−5.06
	ACCT	−8.32	8.02	−2.82	−0.63	−1.36	−5.12
	ACCQ	−8.33	8.00	−2.84	−0.63	−1.36	−5.16
	ACC5	−8.33	8.00	−2.84	−0.63	−1.36	−5.16
	ACC6	−8.33	8.00	−2.84	−0.63	−1.36	−5.16

TABLE 2 The LMO-EDA results of benzene dimer and water dimer at the MP2/CCX and MP2/ACCX level. Energy unit is kcal/mol

MP2		ΔE^{elec}	ΔE^{exrep}	ΔE^{pol}	ΔE^{corr}	ΔE^{TOT}
Benzene dimer	CCD	−3.69	8.43	−1.12	−4.89	−1.27
	CCT	−3.59	8.50	−1.23	−6.58	−2.90
	CCQ	−3.56	8.52	−1.25	−7.14	−3.43
	CC5	−3.54	8.53	−1.26	−7.36	−3.63
	CC6	−3.54	8.53	−1.26	−7.43	−3.70
	ACCD	−3.58	8.57	−1.24	−6.65	−2.91
	ACCT	−3.55	8.54	−1.26	−7.23	−3.50
	ACCQ	−3.54	8.54	−1.26	−7.39	−3.66
Water dimer	CCD	−9.18	7.58	−2.14	−0.25	−4.00
	CCT	−8.60	7.30	−2.31	−0.88	−4.49
	CCQ	−8.48	7.20	−2.35	−1.14	−4.78
	CC5	−8.43	7.15	−2.38	−1.26	−4.91
	CC6	−8.42	7.15	−2.38	−1.31	−4.96
	ACCD	−8.45	7.17	−2.33	−0.80	−4.42
	ACCT	−8.40	7.16	−2.37	−1.14	−4.75
	ACCQ	−8.41	7.15	−2.38	−1.27	−4.92
	ACC5	−8.41	7.15	−2.38	−1.32	−4.97
	ACC6	−8.41	7.15	−2.38	−1.35	−4.99

benzene, water and ammonia water dimers, the geometries were optimized by the B3LYP-D3(BJ) level; for PLY dimer, the geometry was optimized by BS-UωB97X-D; for the triple bonding complexes N_2, P_2, As_2, CO, NO, CH ≡ CH, La_2 and Ac_2, the geometries were optimized with PBE functional.

For benzene and water dimers, a series of Dunning-type correlation consistent basis sets, cc-pVXZ and aug-cc-pVXZ (X = D, T, Q, 5, and 6, denoted as CCX and ACCX in this article),[77] are employed. For the IYQYGG segment, 6-31G basis set is used. For the dissociation curve of ammonia-water dimer, ACCD is employed. For PLY and BTA·

dimers, 6–311++G(d,p) is used. For N_2, P_2, As_2, CO, NO, and CH ≡ CH complexes, CCT is used, while for La_2, Ac_2, and H_3 PAc ≡ $AcPH_3$ complexes, Jorge-TZP basis set[78] is used.

4.1 | Typical van der Waals and hydrogen bonding interactions

Here typical non-covalent interactions are used to show the performance of GKS-EDA/LMO-EDA. The GKS-EDA and LMO-EDA results of the T-shaped benzene dimer and water dimer are shown in Tables 1 and 2, respectively. As for the total interaction energies, the B3LYP-D3 results are in agreement with the results of CCSD(T) in the literature,[22,79] while the MP2 results depend on the size of basis set. For example, the interaction energy of benzene dimer was −2.61 kcal/mol by CCSD(T)/ACCQ,[79] compared to the B3LYP-D3 results from −2.16 to −2.29 kcal/mol, and the MP2 results from −1.27 to −3.70 kcal/mol.

For the EDA results, it is found that the complete basis set (CBS) limit can be reached gradually with the enlargement of basis set. All the GKS-EDA terms and most of LMO-EDA terms are quite stable with the different basis sets, while the correlation term in LMO-EDA shows largely basis set dependent. It is interesting that the values of ΔE^{ele}, ΔE^{exrep}, and ΔE^{pol} in GKS-EDA are close to the corresponding terms in LMO-EDA. The main

difference between the GKS-EDA and LMO-EDA results are contributed by ΔE^{disp} and ΔE^{corr}. With the approximately same total interaction energies, GKS-EDA, and LMO-EDA provide the similar analysis results, showing that the interaction in benzene dimer is dominated by dispersion interaction; while the hydrogen bond in the water dimer is governed by the electrostatic term.

The CPU time and memory consumptions of XEDA calculations for benzene dimer are shown in Table S1. It can be seen that the CPU time consumption and memory costs of GKS-EDA and LMO-EDA are close to the cost for the single point energy (SPE) of supermolecule. For the GKS-EDA calculations of benzene dimer, the CPU time and memory consumptions are about four times and two times consumptions of SPE, respectively. The CPU time is consumed mainly in the orbital module, which provides the monomer and complex's wavefunction via the SCF procedure. For LMO-EDA calculations at the HF level, the CPU time and memory consumptions are similar to that of GKS-EDA. The comparison of the consumptions of XEDA and GAMESS is demonstrated in Figure S1. It can be found that the efficiency of XEDA is greatly improved compared to the EDA module in GAMESS.

4.2 | Two body and many body interactions in IYQYGG segment

Here we show the capability of XEDA for large systems when GKS-EDA is applied. Owning to the low computational scaling with the satisfactory accuracy, GKS-EDA is able to treat the intermolecular interactions of large systems. The IYQYGG segment is an ordered sequence of organic molecular pairs, which can be divided into upper and lower parts.[70] Two body interaction of the IYQYGG segment between the upper and the lower parts, denoted as $(C_{33}H_{45}O_{10}N_7)_{10}$ ...$(C_{33}H_{45}O_{10}N_7)_{10}$, which contains 1900 atoms, is explored by GKS-EDA and shown in Figure 3. As can be seen, the total interaction energy, −302.89 kcal/mol, is dominated by the electrostatic term of −367.32 kcal/mol. Dispersion is also large while polarization and correlation are relatively small.

Furthermore, XEDA is advantageous for exploring the origin of many body effects. The GKS-EDA results for the many body interactions in the tetramer $(C_{33}H_{45}O_{10}N_7)_4$ are shown in Table 3. It is found
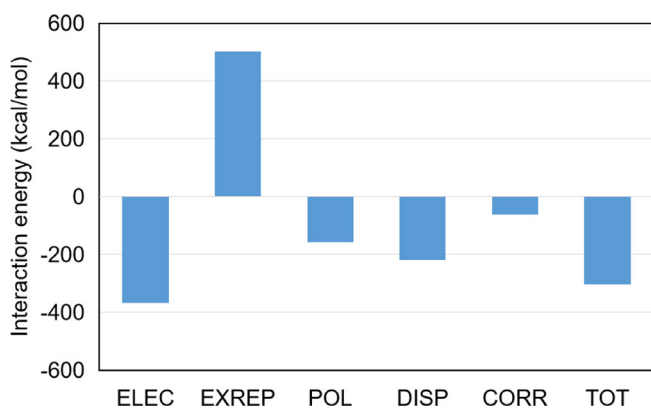

FIGURE 3 The GKS-EDA result of the two-body interaction of $(C_{33}H_{45}O_{10}N_7)_{10}$...$(C_{33}H_{45}O_{10}N_7)_{10}$ at the B3LYP-D3/6-31G level

TABLE 3 The GKS-EDA results of the four-body interaction in $(C_{33}H_{45}O_{10}N_7)_4$ at B3LYP-D3/6-31G level without BSSE correction. Energy unit is kcal/mol
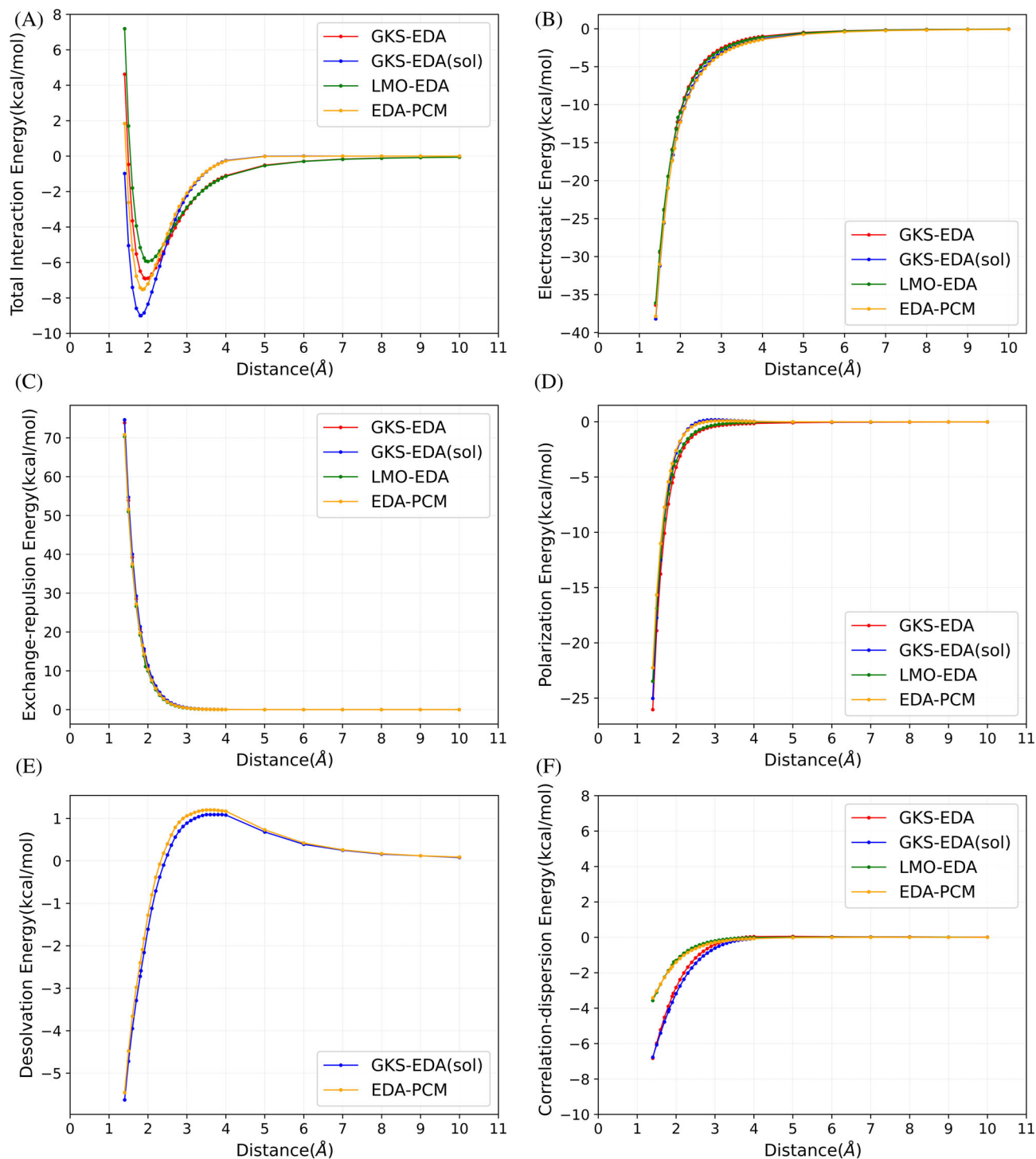
Interaction	ΔE^{elec}	ΔE^{exrep}	ΔE^{pol}	ΔE^{disp}	ΔE^{corr}	ΔE^{TOT}
1 versus 2	−58.38	68.63	−38.27	−41.03	−15.50	−84.55
1 versus 3	−14.78	20.29	−8.68	−10.84	−4.51	−18.50
1 versus 4	−14.76	20.30	−8.64	−10.85	−4.49	−18.44
2 versus 3	−14.76	20.30	−8.64	−10.85	−4.34	−18.28
2 versus 4	−0.06	0	0.05	−0.61	−0.12	−0.75
3 versus 4	−58.24	68.63	−38.25	−41.03	−15.44	−84.33
Sum of above (ΔE_{sum})	−160.98	198.16	−102.43	−115.21	−44.39	−224.85
Four-body interaction (ΔE_{all})	−160.98	197.83	−103.70	−115.19	−44.26	−226.30
Many body effects ($\Delta\Delta E$)	0	−0.33	−1.27	0.02	0.14	−1.45

FIGURE 4 The GKS-EDA(sol) and EDA-PCM results of the potential energy surface of NH_3–H_2O in aqueous solution. [a] (a) Total interaction energy; (b) electrostatic term; (c) exchange-repulsion term; (d) polarization term; (e) desolvation term; (f) correlation-dispersion term for GKS-EDA and correlation term for LMO-EDA

that the total tetramer interaction energy is controlled by electrostatic and dispersion terms. Among the 62 body interactions, the interactions between fragments 1 and 2, fragments 3 and 4 are the largest, showing that the left–right part interactions are stronger than the upper-lower parts. Without BSSE correction, the sums of electrostatic

and dispersion terms in two fragment interactions are exactly equal to those of the total tetramer interaction. As can be seen, the many body effects are mainly contributed by the polarization term.

The CPU time and memory costs of GKS-EDA for $(C_{33}H_{45}O_{10}N_7)_n$...$(C_{33}H_{45}O_{10}N_7)_n$ ($n = 1$–10) are shown in Table S2. The results are similar

to those of benzene dimer in Table S1, showing that the costs are the same order of magnitude to those of SPE calculations. According to

Table S2, about 40–60% of the total time can be saved when the optimized monomer and complex's wavefunction is provided (which means that the SCF procedure can be skipped).
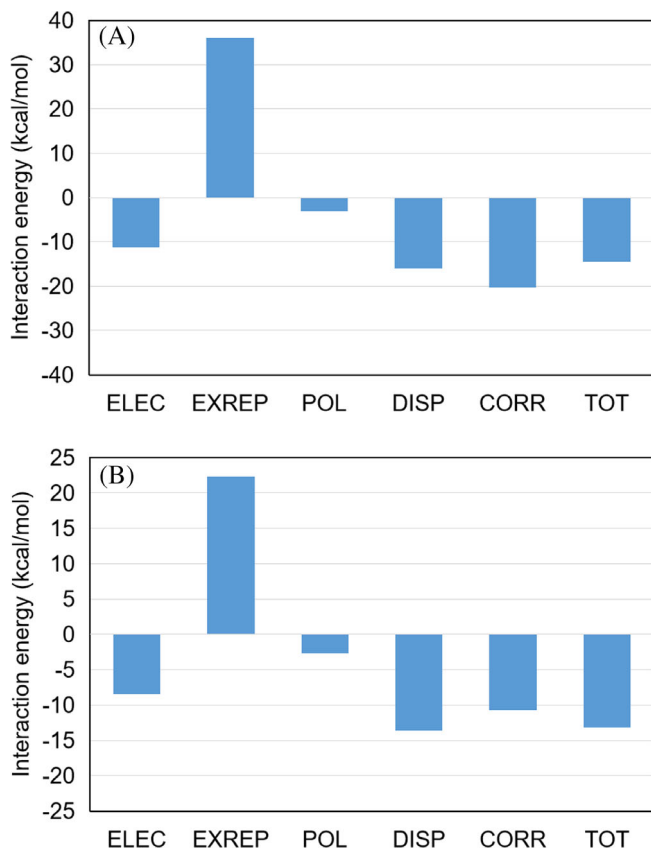

FIGURE 5 The GKS-EDA(BS) results for radical–radical interactions at the ωB97X-D/6-311++G(d,p) level. (A) PLY dimer; (B) BTA· dimer

4.3 | Potential energy surface of $NH_3...H_2O$ in aqueous solution

Here we show the capability of XEDA for intermolecular interactions in solvation environment. The potential energy surfaces (PES) and the curves of the individual EDA terms of the $NH_3...H_2O$ hydrogen bond (HB) in aqueous solution, which are obtained by GKS-EDA(sol) and EDA-PCM, are shown in Figure 4. For comparison, the results of GKS-EDA and LMO-EDA are also listed.

The origin of the hydrogen bond in aqueous solution is similar to the gas phase one, indicating that the electrostatic interaction is dominant, followed by the polarization term. In general, different from the HBs in water dimer and HF dimer,[24] the HB in $NH_3...H_2O$ around the equilibrium bond distance is enhanced by the solvent effects. It can be attributed by the increase of electrostatic interaction and the negative desolvation energy at the short distance. Moreover, it is found that all the curves are smooth in the whole surface, indicating that the total interaction energy and EDA terms change continuously with the variation of the bonding distance.

4.4 | Radical–radical interactions in phenalenyl dimer and bis-dithiazolyl radical dimer

Intermolecular interactions with OSS states possess multi-reference characters, which are challenging for single-determinant based EDA methods. This kind of interactions can be treated by GKS-EDA(BS).

TABLE 4 The GKS-EDA results of the triple bonds. Energy unit is kcal/mol

	Multiplicity of each fragment	Level	ΔE^{elec}	ΔE^{exrep}	ΔE^{pol}	ΔE^{corr}	ΔE^{TOT}
N_2	$N(^4A)...N(^4A)$	UPBE/CCT	−318.29	817.39	−607.40	−134.55	−242.85
		ROPBE/CCT	−318.43	829.26	−622.46	−132.61	−244.24
P_2	$P(^4A)...P(^4A)$	UPBE/CCT	−181.52	339.45	−188.41	−90.97	−121.45
		ROPBE/CCT	−181.53	339.84	−189.09	−90.98	−121.76
As_2	$As(^4A)...As(^4A)$	UPBE/CCT	−178.51	299.15	−124.44	−93.89	−97.68
		ROPBE/CCT	−178.61	299.11	−125.54	−93.33	−98.37
$CH \equiv CH$	$CH(^4A)...CH(^4A)$	UPBE/CCT	−142.19	233.85	−259.32	−107.19	−274.85
		ROPBE/CCT	−141.28	234.52	−262.67	−106.33	−275.76
CO	$C(^3A)...O(^3A)$	UPBE/CCT	−287.01	791.88	−672.06	−101.23	−268.43
		ROPBE/CCT	−296.05	809.88	−689.36	−98.19	−273.72
NO	$N(^4A)...O(^3A)$	UPBE/CCT	−229.75	643.47	−456.60	−128.83	−171.72
		ROPBE/CCT	−229.66	651.47	−470.28	−127.35	−175.81
La_2	$La(^4A)...La(^4A)$	UPBE/Jorge-TZP	−147.28	282.65	−105.16	−77.36	−47.14
		ROPBE/Jorge-TZP	−147.14	282.37	−107.62	−75.52	−47.90
Ac_2	$Ac(^4A)...Ac(^4A)$	UPBE/Jorge-TZP	−415.57	563.35	−121.02	−85.18	−58.43
		ROPBE/Jorge-TZP	−416.66	564.33	−122.84	−83.92	−59.09

Phenalenyl (PLY) is a kind of polycyclic aromatic hydrocarbons with a single occupied HOMO. There exists a radical–radical interaction in PLY dimer, which has been studied extensively.[80–84] The GKS-EDA (BS) result of PLY dimer at the U-ωB97X-D/6-311++G(d,p) level is shown in Figure 5(A). It is shown that the interaction is dominated by the correlation term. The result of 6-311++G(d,p) is almost the same as that of the smaller basis set 6-31+G(d) in literature,[33] showing the basis set independence of GKS-EDA(BS).

The GKS-EDA(BS) result of the BTA· radical dimer is shown in Figure 5(B). The total interaction energy is similar to the value in literature.[85] It is shown that similar to PLY dimer, correlation and dispersion terms are the most important for the radical–radical interactions. Different from PLY dimer, dispersion term in BTA· dimer is somewhat larger than correlation term. Polarization term in PLY dimer and BTA· dimer is always small, showing the weak covalent character of radical–radical interaction.

4.5 | Triple bonds in typical diatomic molecules and transit metal complexes

Besides the non-covalent interactions discussed above, XEDA is capable of handling strong covalent bonds. The GKS-EDA results of the triple bonds, including N_2, P_2, As_2, CO, NO, $CH \equiv CH$, La_2, and Ac_2, are shown in Table 4. The LMO-EDA results, and EDA-NOCV results taken from literature[86] are shown in Table S3 of supporting information, which are generally similar to the GKS-EDA ones. It is noted that in EDA-NOCV, the contribution of correlation, which is not explicitly expressed, is included in electrostatic and orbital terms. To describe the triple bonds, the spin state of each monomer (or atom) should be set as quadruplet or triplet state, which can be handled by unrestricted or restricted open type of wavefunction. In general, the GKS-EDA results with unrestricted orbitals are similar to those with restricted open shell orbitals. As can be seen from Table 4, the typical triple bonds by the first row main group elements, acetylene, CO, NO, and N_2, polarization term is the largest while electrostatic is the secondary. The polarization of CO is larger than that of N_2. It makes sense because of the lone pair resonance from O atom to C atom. For acetylene, given the small polarization and electrostatic terms, the lowest exchange-repulsion term leads to the largest total interaction energy. For P_2, the main contribution of the triple bond is the polarization and electrostatic terms, which are almost equal. As for As_2, La_2, and Ac_2, their total interaction energies are dominant by electrostatic term, followed by polarization. It is noted that the proportion of correlation term in La_2 and Ac_2 is large compared to those in the other complexes.

The GKS-EDA results of different bond breaking modes of $H_3PAc \equiv AcPH_3$, which are shown in Table S4, can be compared with the EDA-NOCV results from literature.[87] Given the similar total binding energies, GKS-EDA and EDA-NOCV both show that electrostatic term and polarization (orbital interaction) have large contributions to the total interaction energy. However, GKS-EDA gives a large correlation term which is not presented in EDA-NOCV.

5 | CONCLUSION

In this article, a new energy decomposition analysis program, called XEDA, is introduced. The program employs LMO-EDA and GKS-EDA and their extensions, to explore the physical origin of intermolecular interactions. The memory and time consumptions are the same level of SPE calculations. Test examples show that XEDA is able to analyze various intermolecular interactions, ranging from weak interactions (van der Waals, hydrogen bond, etc) to strong covalent bonds (triple bonds), from gas phase to condensed phase, from closed-shell to open-shell molecules. Further development of XEDA will focus on high computational efficiency and strong correlation in complex systems.

DATA AVAILABILITY STATEMENT

The data that support the findings of this study are available within this article and its supplementary material (including Tables S1–S4, and Figure S1).

ORCID

Wei Wu https://orcid.org/0000-0002-6139-5443
Peifeng Su https://orcid.org/0000-0003-4398-6888

REFERENCES

[1] E. Francisco, A. M. Pendás, in *Non-covalent Interactions in Quantum Chemistry and Physics: Theory and Applications* (Eds: A. O. de la Roza, G. A. DiLabio), Elsevier, Amsterdam **2017**, p. 27.
[2] E. Pastorczak, C. Corminboeuf, *J. Chem. Phys.* **2017**, *146*, 120901.
[3] J. Andres, P. W. Ayers, R. A. Boto, R. Carbo-Dorca, H. Chermette, J. Cioslowski, J. Contreras-Garcia, D. L. Cooper, G. Frenking, C. Gatti, F. Heidar-Zadeh, L. Joubert, A. Martin Pendas, E. Matito, I. Mayer, A. J. Misquitta, Y. Mo, J. Pilme, P. L. A. Popelier, M. Rahm, E. Ramos-Cordoba, P. Salvador, W. H. E. Schwarz, S. Shahbazian, B. Silvi, M. Sola, K. Szalewicz, V. Tognetti, F. Weinhold, E. L. Zins, *J. Comput. Chem.* **2019**, *40*, 2248.
[4] B. Jeziorski, R. Moszynski, K. Szalewicz, *Chem. Rev.* **1994**, *94*, 1887.
[5] K. Szalewicz, *WIREs Comput. Mol. Sci.* **2012**, *2*, 254.
[6] E. G. Hohenstein, C. D. Sherrill, *WIREs Comput. Mol. Sci.* **2012**, *2*, 304.
[7] G. Jansen, *WIREs Comput. Mol. Sci.* **2014**, *4*, 127.
[8] K. Patkowski, *WIREs Comput. Mol. Sci.* **2019**, *10*, e1452.
[9] M. J. Phipps, T. Fox, C. S. Tautermann, C. K. Skylaris, *Chem. Soc. Rev.* **2015**, *44*, 3177.
[10] L. Zhao, M. von Hopffgarten, D. M. Andrada, G. Frenking, *WIREs Comput. Mol. Sci.* **2018**, *8*, e1345.
[11] P. Su, Z. Tang, W. Wu, *WIREs Comput. Mol. Sci.* **2020**, *10*, e1460.

[12] Y. Mao, M. Loipersberger, P. R. Horn, A. Das, O. Demerdash, D. S. Levine, S. Prasad Veccham, T. Head-Gordon, M. Head-Gordon, *Annu. Rev. Phys. Chem.* **2021**, *72*, 641.

[13] K. Kitaura, K. Morokuma, *Int. J. Quantum Chem.* **1976**, *10*, 325.

[14] T. Ziegler, A. Rauk, *Theoret. Chim. Acta* **1977**, *46*, 1.

[15] T. Ziegler, A. Rauk, *Inorg. Chem.* **1979**, *18*, 1755.

[16] T. Ziegler, A. Rauk, *Inorg Chem* **1979**, *18*, 1558.

[17] W. J. Stevens, W. H. Fink, *Chem. Phys. Lett.* **1987**, *139*, 15.

[18] W. Chen, M. S. Gordon, *J. Phys. Chem.* **1996**, *100*, 14316.

[19] Y. Mo, J. Gao, S. D. Peyerimhoff, *J. Chem. Phys.* **2000**, *112*, 5530.

[20] R. Z. Khaliullin, E. A. Cobar, R. C. Lochan, A. T. Bell, M. Head-Gordon, *J. Phys. Chem. A* **2007**, *111*, 8753.

[21] M. P. Mitoraj, A. Michalak, T. Ziegler, *J. Chem. Theory Comput.* **2009**, *5*, 962.

[22] P. Su, H. Li, *J. Chem. Phys.* **2009**, *131*, 14102.

[23] Y. Mo, P. Bao, J. Gao, *Phys. Chem. Chem. Phys.* **2011**, *13*, 6760.

[24] P. Su, H. Liu, W. Wu, *J. Chem. Phys.* **2012**, *137*, 34111.

[25] P. Su, Z. Jiang, Z. Chen, W. Wu, *J. Phys. Chem. A* **2014**, *118*, 2531.

[26] P. Su, Z. Chen, W. Wu, *Chem. Phys. Lett.* **2015**, *635*, 250.

[27] W. B. Schneider, G. Bistoni, M. Sparta, M. Saitow, C. Riplinger, A. A. Auer, F. Neese, *J. Chem. Theory Comput.* **2016**, *12*, 4778.

[28] P. Su, H. Chen, W. Wu, *Sci. China Chem.* **2016**, *59*, 1025.

[29] A. Altun, F. Neese, G. Bistoni, *Beilstein J. Org. Chem.* **2018**, *14*, 919.

[30] Q. Ge, M. Head-Gordon, *J. Chem. Theory Comput.* **2018**, *14*, 5156.

[31] Q. Ge, Y. Mao, M. Head-Gordon, *J. Chem. Phys.* **2018**, *148*, 64105.

[32] A. Altun, F. Neese, G. Bistoni, *J. Chem. Theory Comput.* **2019**, *15*, 215.

[33] Z. Tang, Z. Jiang, H. Chen, P. Su, W. Wu, *J. Chem. Phys.* **2019**, *151*, 244106.

[34] Y. Mao, D. S. Levine, M. Loipersberger, P. R. Horn, M. Head-Gordon, *Phys. Chem. Chem. Phys.* **2020**, *22*, 12867.

[35] M. A. Blanco, A. Martín Pendás, E. Francisco, *J. Chem. Theory Comput.* **2005**, *1*, 1096.

[36] E. Francisco, A. Martín Pendás, M. A. Blanco, *J. Chem. Theory Comput.* **2006**, *2*, 90.

[37] A. Martín Pendás, M. A. Blanco, E. Francisco, *J. Comput. Chem.* **2007**, *28*, 161.

[38] G. M. J. Barca, C. Bertoni, L. Carrington, D. Datta, N. De Silva, J. E. Deustua, D. G. Fedorov, J. R. Gour, A. O. Gunina, E. Guidez, T. Harville, S. Irle, J. Ivanic, K. Kowalski, S. S. Leang, H. Li, W. Li, J. J. Lutz, I. Magoulas, J. Mato, V. Mironov, H. Nakata, B. Q. Pham, P. Piecuch, D. Poole, S. R. Pruitt, A. P. Rendell, L. B. Roskop, K. Ruedenberg, T. Sattasathuchana, M. W. Schmidt, J. Shen, L. Slipchenko, M. Sosonkina, V. Sundriyal, A. Tiwari, J. L. Galvez Vallejo, B. Westheimer, M. Włoch, P. Xu, F. Zahariev, M. S. Gordon, *J. Chem. Phys.* **2020**, *152*, 154102.

[39] G. te Velde, F. M. Bickelhaupt, E. J. Baerends, C. Fonseca Guerra, S. J. A. van Gisbergen, J. G. Snijders, T. Ziegler, *J. Comput. Chem.* **2001**, *22*, 931.

[40] Y. I. Shao, Z. Gan, E. Epifanovsky, A. T. B. Gilbert, M. Wormit, J. Kussmann, A. W. Lange, A. Behn, J. Deng, X. Feng, D. Ghosh, M. Goldey, P. R. Horn, L. D. Jacobson, I. Kaliman, R. Z. Khaliullin, T. Kuś, A. Landau, J. Liu, E. I. Proynov, Y. M. Rhee, R. M. Richard, M. A. Rohrdanz, R. P. Steele, E. J. Sundstrom, H. L. Woodcock, P. M. Zimmerman, D. Zuev, B. Albrecht, E. Alguire, B. Austin, G. J. O. Beran, Y. A. Bernard, E. Berquist, K. Brandhorst, K. B. Bravaya, S. T. Brown, D. Casanova, C.-M. Chang, Y. Chen, S. H. Chien, K. D. Closser, D. L. Crittenden, M. Diedenhofen, R. A. DiStasio, H. Do, A. D. Dutoi, R. G. Edgar, S. Fatehi, L. Fusti-Molnar, A. Ghysels, A. Golubeva-Zadorozhnaya, J. Gomes, M.s W. D. Hanson-Heine, P. H. P. Harbach, A. W. Hauser, E. G. Hohenstein, Z. C. Holden, T.-C. Jagau, H. Ji, B. Kaduk, K. Khistyaev, J. Kim, J. Kim, R. A. King, P. Klunzinger, D. Kosenkov, T. Kowalczyk, C. M. Krauter, K. U. Lao, A. D. Laurent, K. V. Lawler, S. V. Levchenko, C. Y. Lin, F. Liu, E. Livshits, R. C. Lochan, A. Luenser, P. Manohar, S. l. F. Manzer, S.-P. Mao, N. Mardirossian, A. V. Marenich, S. A. Maurer, N. J. Mayhall, E. Neuscamman, C. M. Oana, R. Olivares-Amaya, D. P. O'Neill, J. A. Parkhill, T. M. Perrine, R. Peverati, A. Prociuk, D. R. Rehn, E. Rosta, N. J. Russ, S. M. Sharada, S. Sharma, D. W. Small, A. Sodt, T. Stein, D. Stück, Y.-C. Su, A. J. W. Thom, T. Tsuchimochi, V. Vanovschi, L. Vogt, O. Vydrov, T. Wang, M. A. Watson, J. Wenzel, A. White, C.r F. Williams, J. Yang, S. Yeganeh, S. R. Yost, Z. Q. You, I. Y. Zhang, X. Zhang, Y. Zhao, B. R. Brooks, G. K. L. Chan, D. M. Chipman, C. J. Cramer, W. A. Goddard, M. S. Gordon, W. J. Hehre, A. Klamt, H. F. Schaefer, M. W. Schmidt, C. D. Sherrill, D. G. Truhlar, A. Warshel, X. Xu, A. Aspuru-Guzik, R. Baer, A. T. Bell, N. A. Besley, J.-D. Chai, A. Dreuw, B. D. Dunietz, T. R. Furlani, S. R. Gwaltney, C.-P. Hsu, Y. Jung, J. Kong, D. S. Lambrecht, W. Liang, C. Ochsenfeld, Vi. A. Rassolov, L. V. Slipchenko, J. E. Subotnik, T. Van Voorhis, J. M. Herbert, A. I. Krylov, P. M. W. Gill, M. Head-Gordon, *Mol. Phys.* **2015**, *113*, 184.

[41] F. Neese, F. Wennmohs, U. Becker, C. Riplinger, *J. Chem. Phys.* **2020**, *152*, 224108.

[42] D. G. A. Smith, L. A. Burns, A. C. Simmonett, R. M. Parrish, M. C. Schieber, R. Galvelis, P. Kraus, H. Kruse, R. Di Remigio, A. Alenaizan, A. M. James, S. Lehtola, J. P. Misiewicz, M. Scheurer, R. A. Shaw, J. B. Schriber, Y. Xie, Z. L. Glick, D. A. Sirianni, J. S. O'Brien, J. M. Waldrop, A. Kumar, E. G. Hohenstein, B. P. Pritchard, B. R. Brooks, H. F. Schaefer, A. Y. Sokolov, K. Patkowski, A. E. DePrince, U. Bozkaya, R. A. King, F. A. Evangelista, J. M. Turney, T. D. l. Crawford, C. D. Sherrill, *J. Chem. Phys.* **2020**, *152*, 184108.

[43] H.-J. Werner, P. J. Knowles, F. R. Manby, J. A. Black, K. Doll, A. Heßelmann, D. Kats, A. Köhn, T. Korona, D. A. Kreplin, Q. Ma, T. F. Miller, A. Mitrushchenkov, K. A. Peterson, I. Polyak, G. Rauhut, M. Sibaev, *J. Chem. Phys.* **2020**, *152*, 144107.

[44] Misquitta, A. J., Stone, A. **2016**. http://www-stone.ch.cam.ac.uk/programs.html#CamCASP.

[45] J. Garcia, R. Podeszwa, K. Szalewicz, *J. Chem. Phys.* **2020**, *152*, 184109.

[46] S. G. Balasubramani, G. P. Chen, S. Coriani, M. Diedenhofen, M. S. Frank, Y. J. Franzke, F. Furche, R. Grotjahn, M. E. Harding, C. Hättig, A. Hellweg, B. Helmich-Paris, C. Holzer, U. Huniar, M. Kaupp, A. Marefat Khah, S. Karbalaei Khani, T. Müller, F. Mack, B. D. Nguyen, S. M. Parker, E. Perlt, D. Rappoport, K. Reiter, S. Roy, M. Rückert, G. Schmitz, M. Sierka, E. Tapavicza, D. P. Tew, C. van Wüllen, V. K. Voora, F. Weigend, A. Wodyński, J. M. Yu, *J. Chem. Phys.* **2020**, *152*, 184107.

[47] C. Sukpattanacharoen, P. Kumar, Y. Chi, N. Kungwan, D. Escudero, *Inorg. Chem.* **2020**, *59*, 18253.

[48] A. Seidl, A. Görling, P. Vogl, J. A. Majewski, M. Levy, *Phys. Rev. B* **1996**, *53*, 3764.

[49] R. Baer, E. Livshits, U. Salzner, *Annu. Rev. Phys. Chem.* **2010**, *61*, 85.

[50] K. Yamaguchi, Y. Takahara, T. Fueno, in *Applied Quantum Chemistry* (Eds: V. H. Smith, H. F. Schaefer, K. Morokuma), D. Reidel Publishing Company, Dordrecht, Holland **1986**, p. 155.

[51] F. Neese, *J. Phys. Chem. Solids* **2004**, *65*, 781.

[52] C. Møller, M. S. Plesset, *Phys. Rev.* **1934**, *46*, 618.

[53] R. J. Bartlett, G. D. Purvis, *Int. J. Quantum Chem.* **1978**, *14*, 561.

[54] J. A. Pople, R. Krishnan, H. B. Schlegel, J. S. Binkley, *Int. J. Quantum Chem.* **1978**, *14*, 545.

[55] J. G. Kirkwood, *J. Chem. Phys.* **1934**, *2*, 351.

[56] L. Onsager, *J. Am. Chem. Soc.* **1936**, *58*, 1486.

[57] O. Tapia, O. Goscinski, *Mol. Phys.* **1975**, *29*, 1653.

[58] R. Cammi, J. Tomasi, *J. Comput. Chem.* **1995**, *16*, 1449.

[59] S. Miertuš, E. Scrocco, J. Tomasi, *Chem. Phys.* **1981**, *55*, 117.

[60] S. Miertusč, J. Tomasi, *Chem. Phys.* **1982**, *65*, 239.

[61] V. Barone, M. Cossi, *J. Phys. Chem. A* **1998**, *102*, 1995.

[62] M. Cossi, N. Rega, G. Scalmani, V. Barone, *J. Comput. Chem.* **2003**, *24*, 669.

[63] E. Cancès, B. Mennucci, *J. Chem. Phys.* **1998**, *109*, 249.

[64] E. Cancès, B. Mennucci, J. Tomasi, *J. Chem. Phys.* **1998**, *109*, 260.

[65] M. Cossi, V. Barone, *J. Chem. Phys.* **1998**, *109*, 6246.

[66] B. Mennucci, R. Cammi, J. Tomasi, *J. Chem. Phys.* **1999**, *110*, 6858.

[67] D. Si, H. Li, *J. Chem. Phys.* **2009**, *131*, 044123.

[68] A. V. Marenich, C. J. Cramer, D. G. Truhlar, *J. Phys. Chem. B* **2009**, *113*, 6378.

[69] Landau, M., Perov, S., **2019**, doi: https://doi.org/10.2210/pdb6G8C/pdb.

[70] S. Perov, O. Lidor, N. Salinas, N. Golan, E. Tayeb-Fligelman, M. Deshmukh, D. Willbold, M. Landau, *PLoS Pathog.* **2019**, *15*, e1007978.

[71] A. D. Becke, *J. Chem. Phys.* **1993**, *98*, 5648.

[72] S. Grimme, S. Ehrlich, L. Goerigk, *J. Comput. Chem.* **2011**, *32*, 1456.

[73] J. D. Chai, M. Head-Gordon, *Phys. Chem. Chem. Phys.* **2008**, *10*, 6615.

[74] J. P. Perdew, K. Burke, M. Ernzerhof, *Phys. Rev. Lett.* **1997**, *78*, 1396.

[75] S. F. Boys, F. Bernardi, *Mol. Phys.* **1970**, *19*, 553.

[76] M. J. Frisch, G. W. Trucks, H. B. Schlegel, G. E. Scuseria, M. A. Robb, J. R. Cheeseman, G. Scalmani, V. Barone, G. A. Petersson, H. Nakatsuji, X. Li, M. Caricato, A. Marenich, J. Bloino, B. G. Janesko, R. Gomperts, B. Mennucci, H. P. Hratchian, J. V. Ortiz, A. F. Izmaylov, J. L. Sonnenberg, D. Williams-Young, F. Ding, F. Lipparini, F. Egidi, J. Goings, B. Peng, A. Petrone, T. Henderson, D. Ranasinghe, V. G. Zakrzewski, J. Gao, N. Rega, G. Zheng, W. Liang, M. Hada, M. Ehara, K. Toyota, R. Fukuda, J. Hasegawa, M. Ishida, T. Nakajima, Y. Honda, O. Kitao, H. Nakai, T. Vreven, K. Throssell, J. A. Montgomery, Jr., J. E. Peralta, F. Ogliaro, M. Bearpark, J. J. Heyd, E. Brothers, K. N. Kudin, V. N. Staroverov, T. Keith, R. Kobayashi, J. Normand, K. Raghavachari, A. Rendell, J. C. Burant, S. S. Iyengar, J. Tomasi, M. Cossi, J. M. Millam, M. Klene, C. Adamo, R. Cammi, J. W. Ochterski, R. L. Martin, K. Morokuma, O. Farkas, J. B. Foresman, D. J. Fox, Gaussian 16 Rev. B.01, Wallingford, CT, **2016**.

[77] J. D. Chai, M. Head-Gordon, *J. Chem. Phys.* **2008**, *128*, 84106.

[78] F. E. Jorge, A. Canal Neto, G. G. Camiletti, S. F. Machado, *J. Chem. Phys.* **2009**, *130*, 64108.

[79] M. O. Sinnokrot, C. D. Sherrill, *J. Phys. Chem. A* **2004**, *108*, 10200.

[80] Z. Cui, H. Lischka, H. Z. Beneberu, M. Kertesz, *J. Am. Chem. Soc.* **2014**, *136*, 5539.

[81] F. Gao, R. Zhong, H. Xu, Z. Su, *J. Phys. Chem. C* **2017**, *121*, 3765.

[82] K. Goto, T. Kubo, K. Yamamoto, K. Nakasuji, K. Sato, D. Shiomi, T. Takui, M. Kubota, T. Kobayashi, K. Yakusi, J. Ouyang, *J. Am. Chem. Soc.* **1999**, *121*, 1619.

[83] F. Mota, J. S. Miller, J. J. Novoa, *J. Am. Chem. Soc.* **2009**, *131*, 7699.

[84] S. Suzuki, Y. Morita, K. Fukui, K. Sato, D. Shiomi, T. Takui, K. Nakasuji, *J. Am. Chem. Soc.* **2006**, *128*, 2530.

[85] D. Jose, A. Datta, *Cryst. Growth Des.* **2011**, *11*, 3137.

[86] C. Esterhuysen, G. Frenking, *Theor. Chem. Acc.* **2003**, *111*, 381.

[87] X. C. Xu, X. K. Zhao, H. S. Hu, *Phys. Chem. Chem. Phys.* **2021**, *23*, 10244.

SUPPORTING INFORMATION

Additional supporting information may be found in the online version of the article at the publisher's website.